Distributed Economic Model Predictive Control for the Joint Energy Dispatch of Wind Farms and Run-of-the-River Hydropower Plants

Luca Santosuosso, Simon Camal, Arthur Lett, Guillaume Bontron, Georges Kariniotakis

Distributed Economic Model Predictive Control for the Joint Energy Dispatch of Wind Farms and Run-of-the-River Hydropower Plants

Luca Santosuosso*, Simon Camal*, Arthur Lett†, Guillaume Bontron† and Georges Kariniotakis*
* Center for Processes, Renewable Energy and Energy Systems (PERSEE), MINES Paris PSL, Sophia Antipolis, France
† Compagnie Nationale du Rhône, Lyon, France

***Abstract*—This study addresses the energy dispatch problem of a virtual power plant (VPP) acting as a price-tacker in the day-ahead electricity market. The VPP comprises wind farms and a cascade of run-of-the-river hydropower plants. Even if the storage capacity of the cascade is limited, it can still be exploited to compensate the variability of wind. This implies dispatching the water reservoirs near to real-time, while accounting for complex constraints and various sources of uncertainty. To this aim, we present a control strategy based on economic model predictive control (MPC), which is then decomposed using the auxiliary problem principle. As a distinctive feature, the proposed algorithm is fully-distributed, i.e. no central coordinator is required. Compared to centralized MPC, the distributed algorithm brings a $\sim 10\%$ reduction in the average execution time of the controller. Moreover, the joint operation of hydropower and wind is shown to enhance the economic value of both assets.**

***Index Terms*—Distributed model predictive control, run-of-the-river hydropower, wind power, storage, complex systems**

NOMENCLATURE

In the following, sets and vectors are denoted in **bold**. We use the symbol $\hat{\cdot}$ to denote uncertain parameters, e.g., $\hat{P}^W$.

Sets:

$\boldsymbol{H}$ - set of hydropower systems, indexed by h
$\boldsymbol{K}$ - MPC prediction horizon, indexed by k
$\boldsymbol{T}$ - set of time steps, indexed by t

Variables:

$P_H(h,t)$ - hydropower generation of h in period t (MW)
$Q_{br}(h,t)$ - barrage discharge of h in period t (m^3/s)
$Q_{tr}(h,t)$ - turbines discharge of h in period t (m^3/s)
$Z(h,t)$ - reservoir water level of h in period t (m)
$Z^{max}(h,t)$ - maximum water level of h in period t (m)
$Z^{min}(h,t)$ - minimum water level of h in period t (m)
$\Delta E^{DAM,\uparrow}(t)$ - positive energy imbalance in period t (MWh)
$\Delta E^{DAM,\downarrow}(t)$ - negative energy imbalance in period t (MWh)

Parameters:

$E^{DAM}(t)$ - VPP energy offer in the DAM in period t (MWh)
$P_H^{max}(h)$ - maximum hydropower generation of h (MW)
$\hat{P}_W(t)$ - wind power generation in period t (MW)
$\hat{Q}_e(h,t)$ - external water inflow into h in period t (either from the upstream river or from the river tributaries) (m^3/s)
$Q_{tr}^{max}(h)$ - maximum turbines discharge of h (m^3/s)
$Q_{tr}^{min}(h)$ - minimum turbines discharge of h (m^3/s)
$Q_{br}^{min}(h)$ - minimum barrage discharge of h (m^3/s)
$S(h)$ - surface area of h (m^2)
$\Delta Q_{tr}(h)$ - turbines discharge ramp limit of h (m^3/s)
$\hat{\pi}^{E,\uparrow}(t)$ - penalty price of positive energy imbalances in period t (€/MWh)
$\hat{\pi}^{E,\downarrow}(t)$ - penalty price of negative energy imbalances in period t (€/MWh)
$\tau_{i,j}^{br}$ - time for water propagation from hydropower system i to j via barrage (s)
$\tau_{i,j}^{tr}$ - time for water propagation from hydropower system i to j via turbines (s)

I. INTRODUCTION

Due to the progressive dismantling of conventional generators in favor of renewable energy sources (RES), namely wind and solar power, the optimal dispatch of stochastic resources by means of controllable units has attracted much attention. In this context, the concept of virtual power plant (VPP) was introduced to enhance the economic value of aggregated resources and contribute to a more stable and reliable grid [1]. Numerous studies focus on optimizing VPPs integrating RES and various flexibility sources like batteries, controllable loads, and electric vehicles for market participation [2] and grid support [3]. Among these flexibility sources, hydropower has already demonstrated its ability to increase the economic value of RES, alleviate congestion, and reduce curtailment, thanks to its fast ramping capability and inexpensive fuel [4].

Hydropower plants are broadly classified as reservoir-based and run-of-the-river. Reservoir-based hydropower involves the construction of large reservoirs to store water. In contrast, run-of-the-river generates electricity mainly through natural water flow, with limited storage capability. While several contributions focus on the joint operation of reservoir-based hydropower and RES, less attention is paid to run-of-the-river, despite its critical role in the energy mix of several regions. For example, several European countries have large run-of-the-river shares, such as France (68% of the hydropower generation in 2019), Austria (74%) and Italy (75%) [5]. A study conducted in [6], based on 33 years of daily data (1980-2012) for 12 European regions, found that integrating run-of-the-river into the energy mix would increase RES penetration in all regions, from 1% to 8%. Nonetheless, the limited flexibility of run-of-the-river presents a significant obstacle to its potential role in mitigating RES variability.

Deploying a cascade of run-of-the-river hydropower plants (CRORHP) offers a strategic solution to this issue by enhancing the overall flexibility of the integrated system. Proposed strategies for cascaded hydropower systems aim to optimize their ancillary services provision [7], engagement in day-ahead and frequency regulation markets [8], and enhancement of RES market value [9]. These approaches primarily focus on scheduling the cascaded system for day-ahead or long-term periods, leaving the challenge of short-term energy dispatch unaddressed. Model predictive control (MPC) has been employed to assess the potential of a CRORHP in mitigating short-term fluctuations in solar [10] and wind power [11]. These studies either neglect the involvement of the CRORHP-RES hybrid system in the electricity market or utilize centralized algorithms for managing short-term energy dispatch.

Optimizing the joint dispatch of RES and a CRORHP in the electricity market demands swift decision-making within tight control windows, all while considering complex constraints. This strongly motivates the investigation of distributed optimization techniques. In this context, distributed MPC represents an attractive decomposition coordination algorithm, as it blends the MPC ability to scale to complex problems with long planning horizons and the distributed optimization ability to scale to problems involving the cooperation between multiple agents. Typically, centralized MPC is decomposed with augmented Lagrangian relaxation methods, using either dual decomposition [12] or the alternating direction method of multipliers (ADMM) [13]. However, both dual decomposition and classical ADMM are not fully-distributed methods, as they require a central coordinator to manage the dual variable update step [14]. In recent years, the range of methods stemming from classical ADMM has notably expanded, including various fully-distributed algorithms [15]. These methods have not yet been applied to the joint energy dispatch of cascaded hydropower plants and RES, primarily due to the complex decoupling of both hydraulic relationships and spatial-temporal constraints associated with hydro-RES hybrid systems.

In this study, we tackle the joint dispatch of a CRORHP and wind farms in the day-ahead electricity market (DAM). First, we design a centralized dispatch strategy based on MPC to maximize the aggregator revenue while considering the complex dynamics of the VPP. Then, by integrating the ideas of the auxiliary problem principle (APP) [16] with MPC, we partition the original controller to achieve its distributed form. The key contributions of this paper can be summarized as follows:

- We present a comprehensive VPP model integrating spatial-temporal dynamics and interactions among heterogeneous energy resources. Moreover, in the framework of a collaboration with the French aggregator Compagnie Nationale du Rhône, we consider real operational curves to represent the constraints linked to agricultural, environmental, and other safety requirements of the CRORHP.
- We propose a novel distributed economic MPC algorithm to tackle the join dispatch of a CRORHP and wind farms. By combining the ideas of the APP and MPC, the subproblems within the distributed framework can be concurrently resolved at each control step. This leads to a fully-distributed algorithm (no central coordinator is required), that can efficiently scale in both the temporal and spatial dimensions of the problem.

Simulations are conducted on a case study that mimics part of the VPP operated by Compagnie Nationale du Rhône [17].

A similar analysis is proposed in [18], addressing the scheduling of a cascaded reservoir-based hydropower system across multiple electricity markets. With respect to [18], in this paper we focus on run-of-the-river developments, whose limited storage capacity complicates the ability to enhance RES market value. Also, instead of the ADMM method used in [18], we combine the concepts of the APP and MPC to attain full parallelization of the control algorithm.

The remainder of the article is organized as follows: Section II defines the problem, Section III presents the control algorithm, Section IV discusses the results, and Section V concludes the study.

II. Problem Statement

The goal is to optimize the energy dispatch of a VPP participating in the DAM. The controller receives a hourly energy offering profile, denoted by $E^{DAM}(t)$, computed on the day before. Then, the problem consists in optimizing the mismatch between the day-ahead offering profile and the actual VPP energy production, on a 10 minute basis. This is achieved by the coordinated control of the VPP assets via distributed MPC.

Fig. 1 depicts the VPP: it comprises a cascade of three run-of-the-river hydropower systems (HS1, HS2 and HS3, respectively) and three geographically sparse wind farms. Each hydropower system is composed by a barrage, a small water reservoir and a hydropower plant, linked by water channels. The external water inflow into the CRORHP is given by the inflow from both the upstream river and its tributaries. The proposed formulation excludes grid constraints, which will be addressed in future works. In other words, we assume that the aggregator does not partake in the grid management.

Energy dispatch takes place after market clearing, meaning that the energy price is already known. We assume that by combining information on energy prices with real-time measurements of the electrical grid state, the aggregator can accurately predict the penalty prices associated with imbalances. We assume a dual-pricing settlement scheme [19], where distinct prices are computed for positive imbalances $\Delta E^{DAM,\uparrow} \in \mathbb{R}^+$ (energy injection higher than the energy offer) and negative imbalances $\Delta E^{DAM,\downarrow} \in \mathbb{R}^+$ (energy injection lower than the energy offer). We denote by $\hat{\pi}^{E,\uparrow}$ and $\hat{\pi}^{E,\downarrow}$ the forecasted penalty prices for positive and negative imbalances, respectively. Also wind power and the external water inflow are assumed to be uncertain parameters. Predictions over these two sources of uncertainty are obtained by averaging probabilistic forecasts provided by Compagnie Nationale du Rhône. We employ deterministic models to handle uncertainty. This choice stems from the controller

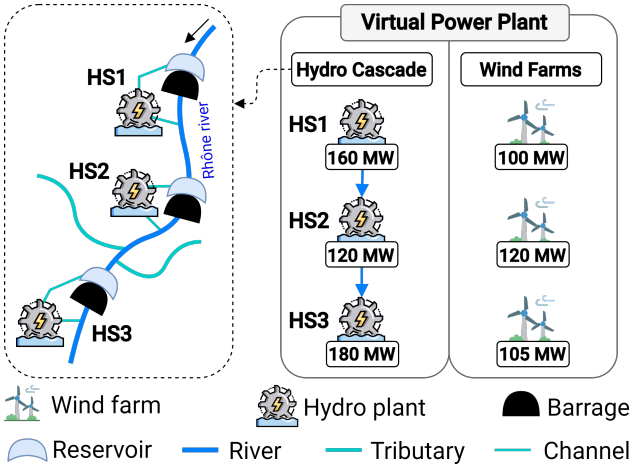

Fig. 1. Diagram of the VPP comprising a CRORHP and wind farms.

need for rapid decision-making and the minimal forecast error expected within the short forecast horizon. Furthermore, incorporating economic key performance indicators directly into the optimization model is anticipated to enhance robustness against uncertainty.

III. Methodology

In this section, we present the system modeling, along with our distributed economic dispatch strategy.

A. Modelling

We model the VPP in Fig. 1 under three key assumptions:

- *Assumption I*. Wind power generation is considered uncontrollable, thereby curtailment or any other action to alter its output is disregarded. This allows a better investigation of the CRORHP ability to mitigate the stochasticity of wind power.
- *Assumption II*. The hydropower generation function is a linear function of the turbines discharge. In general, the hydropower generation depends on both the turbines discharge and the hydraulic head of the reservoir. Nonetheless, during normal inflow conditions, run-of-the-river assets experience minor fluctuations in hydraulic head, allowing to confidently consider it as a constant.
- *Assumption III*. All turbines within each hydropower plant share a common type. Thus, a single variable can be used to represent the cumulative turbines discharge of each asset. Extending our formulation to accommodate the case of diverse turbine types requires minor modifications, which will be included in future works.

In the following, we denote by h a hydropower system in the set of many hydropower systems $\boldsymbol{H}$. Moreover, we present a discrete time problem over a finite set of sampling times $t \in \boldsymbol{T}$ with sampling period Δ_T.

The dynamics of the reservoirs water levels, denoted by Z, are given by:

$$Z(h,t) = Z(h,t-1) + \frac{(Q_{in}(h,t) - Q_{out}(h,t))\Delta_T}{S(h)}, \quad (1)$$

where S denotes the surface area of the reservoir, while Q_{in} and Q_{out} denote the reservoir inflow and outflow, respectively.

In each hydropower system, the reservoir inflow is the sum of three components: the discharge of water from the upstream hydropower system through the barrage and turbines, denoted by Q_{br} and Q_{tr}, respectively, and the uncertain external inflow, denoted by $\hat{Q}_e$. Thus, the total inflow into the h-th reservoir at time t is given by:

$$\begin{aligned} Q_{in}(h,t) =& Q_{br}(h-1, t-\tau^{br}_{h-1,h}) + \\ &+ Q_{tr}(h-1, t-\tau^{tr}_{h-1,h}) + \hat{Q}_e(h,t), \end{aligned} \quad (2)$$

where $\tau^{tr}_{h-1,h}$ and $\tau^{br}_{h-1,h}$ denote the time for water propagation from hydropower system $h-1$ to h via turbines and barrage, respectively. Similarly, the outflow is given by:

$$Q_{out}(h,t) = Q_{br}(h,t) + Q_{tr}(h,t). \quad (3)$$

We rely on historical measurements performed by Compagnie Nationale du Rhône to determine the values of $\tau^{tr}_{h-1,h}$ and $\tau^{br}_{h-1,h}$. During normal inflow conditions, we can safely assume constant water propagation times because of the stable discharge from the hydropower plants. However, during floods, propagation times can fluctuate significantly, depending on the river flow rate.

To ensure stability and safety of the hydropower systems, the CRORHP is operated accordingly to strict operational curves (see Fig. 2).

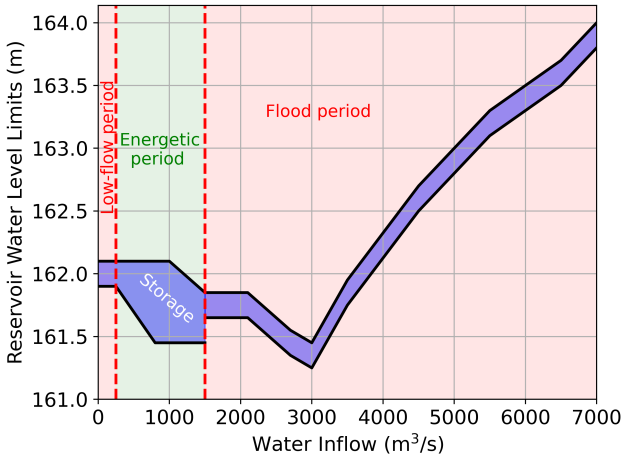

Fig. 2. Example of operational curve of a hydropower system operated by Compagnie Nationale du Rhône [17].

The operational curves are established according to approved guidelines from relevant authorities and are linked to various constraints like navigation, irrigation, nuclear safety, environment, agriculture and tourism. During times of low water flow, i.e., *low-flow periods*, the hydropower system is managed to maintain high water levels to facilitate optimal draught for navigation. Conversely, during *flood periods*, efforts are made to maintain the water levels as close as possible to the natural conditions prior to the barrage construction. Only during normal inflow conditions, i.e., during *energetic periods*, the reservoir provides storage capacity.

To model the operational curves, we compute the minimum and maximum water levels of each reservoir, denoted by $Z^{min}(h,t)$ and $Z^{max}(h,t)$, respectively, as functions of the water inflow. Binary variables are used to provide a piecewise linear approximation of these functions over the aforementioned operational periods.

Specific constraints are included to prevent an excessive wear of the hydraulic equipment. First, the turbines discharge is subject to the ramp limit $|Q_{tr}(h,t) - Q_{tr}(h,t-1)| \leq \Delta Q_{tr}(h)$. Second, the opening of the barrage is allowed only under two conditions: the reservoir is full and the turbines have reached their maximum discharge capacity. Thanks to applying economic-oriented control and under the assumption that energy prices are positive, the optimal solution invariably involves saturating the turbines before opening the barrage. Consequently, we introduce explicit constraints solely to ensure the fulfillment of the former condition. This is given by:

$$Q_{br}(h,t) \leq \begin{cases} 0 & \text{if } Z(h,t) < Z^{max}(h,t) \\ \infty & \text{otherwise} \end{cases}. \tag{4}$$

Binary variables are employed to model (4). When the turbines operate, their discharge must satisfy $Q_{tr}^{min}(h) \leq Q_{tr}(h,t) \leq Q_{tr}^{max}(h)$. When the barrage is open, the barrage discharge must satisfy $Q_{br}(h,t) \geq Q_{br}^{min}(h)$.

Under *Assumption II*, the hydropower generation function, denoted by P_H, is given by:

$$P_H(h,t) = \frac{P_H^{max}(h) Q_{tr}(h,t)}{Q_{tr}^{max}(h)}. \tag{5}$$

Then, the power balance of the VPP is given by:

$$\begin{aligned} E^{DAM}(t) = \left(\sum_{h \in \boldsymbol{H}} P_H(h,t) + \hat{P}_W(t) \right) \Delta_T + \\ - \Delta E^{DAM,\uparrow}(t) + \Delta E^{DAM,\downarrow}(t), \end{aligned} \tag{6}$$

where $\hat{P}_W$ denotes the uncertain wind power generation.

B. Centralized model predictive control

The proposed energy dispatch strategy is formulated as an MPC problem. At time $t \in \boldsymbol{T}$, the MPC receives the energy offering profile and forecasts of the uncertain parameters, for each step of the MPC prediction horizon, i.e., $\forall k \in \boldsymbol{K}$. Then, a sequence of control actions are computed to minimize

$$\begin{aligned} J = \sum_{k \in \boldsymbol{K}} \big(\hat{\pi}^{E,\downarrow}(t+k) \Delta E^{DAM,\downarrow}(t+k|t) + \\ - \hat{\pi}^{E,\uparrow}(t+k) \Delta E^{DAM,\uparrow}(t+k|t) \big), \end{aligned} \tag{7}$$

which represents the total cost of energy imbalances.

Formally, the optimization model solved by the centralized economic MPC strategy (CEMPC) at each time $t \in \boldsymbol{T}$ is:

$$\underset{Q_{tr}(h,t+k|t), Q_{br}(h,t+k|t)}{\operatorname{argmin}} \quad J \tag{8a}$$

$$\text{s.t.} \quad (1)\text{-}(6), \forall h \in \boldsymbol{H}, \forall k \in \boldsymbol{K}, \tag{8b}$$

which is a mixed-integer linear program.

In words, (8) determines the dispatch of the CRORHP that minimizes the cost associated with energy imbalances arising from the variability of the VPP power generation. The optimization model (8) is centralized since its resolution requires the complete information from the VPP resources. By leveraging well known findings from distributed optimization theory, we can break down the centralized problem into smaller problems, which can be solved in parallel until a consensus is achieved on the coupling constraints.

C. From centralized to distributed model predictive control

The centralized problem (8), exhibits two sets of coupling constraints: the reservoir dynamics (1) and the power balance (6). Thus, to reach its fully-distributed form, we undertake a two-step decomposition approach. First, we separate the high-level problem, which involves minimizing the global VPP cost of imbalances subject to the power balance (6), from the low-level problem, which consists in optimizing the CRORHP dispatch. Further breaking down the low-level problem, we achieve a separation between the individual operation of the hydropower systems, subject to to their operational constraints (1)-(5). This sequential decomposition results in the structure depicted in Fig. 3, where the original problem is divided into interconnected components. As each low-level component is associated to a hydropower system, we employ the index $h \in \boldsymbol{H}$ to identify also these components.

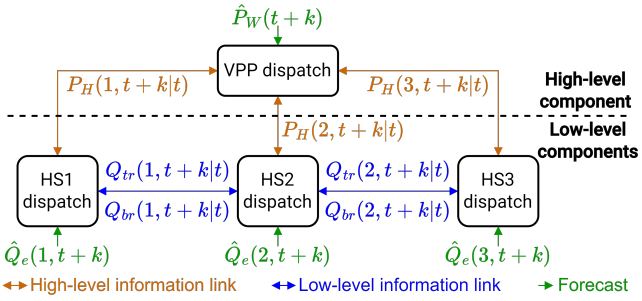

Fig. 3. Structure of the distributed economic MPC strategy.

To ensure coordinated optimization within the distributed structure, the components share two sets of coupling variables: one for the hydropower generation variables, and one for the turbines and barrage discharges. To simplify the following formulation, we group the high-level coupling variables in vector $\boldsymbol{p} = [\boldsymbol{p}_1, \boldsymbol{p}_2, \boldsymbol{p}_3]^T$, where $\boldsymbol{p}_h = [P_H(h,t+1|t), P_H(h,t+2|t), ..., P_H(h,t+K|t)]$, and the low-level coupling variables in $\boldsymbol{q}_h = \left[\boldsymbol{q}_{h,1}, \boldsymbol{q}_{h,2}, ..., \boldsymbol{q}_{h,K}\right]^T$, where $\boldsymbol{q}_{h,k} = [Q_{tr}(h,t+k|t), Q_{br}(h,t+k|t)]$.

Consider again Fig. 3, where each low-level component is connected to its neighbours through low-level information links. The set of coupling variables shared among the low-level component h and its neighbours is $\{\boldsymbol{q}_l \,|\, l \in \boldsymbol{L}_h\}$, where $\boldsymbol{L}_h$ denotes the set of indices associated with the low-level coupling variables of h. Then, we duplicate these variables. We denote by $\bar{\boldsymbol{p}}_h$ and $\bar{\boldsymbol{q}}_l$ the duplicates of $\boldsymbol{p}_h$ and $\boldsymbol{q}_l$, respectively. Since duplicated variables must assume identical values, we

enforce the consistency constraints $\boldsymbol{p}_h = \bar{\boldsymbol{p}}_h$ and $\boldsymbol{q}_l = \bar{\boldsymbol{q}}_l$. We denote by $\boldsymbol{\lambda}_{\boldsymbol{p}_h}$ and $\boldsymbol{\lambda}_{\boldsymbol{q}_l}$ the corresponding vectors of dual variables. Moreover, we collect in vector $\boldsymbol{x}$ the decision variables pertinent only to the high-level problem, namely the energy imbalances, and in $\boldsymbol{y}_h$ those associated only to the low-level component h, namely the reservoirs water levels and the associated binary variables. We denote by $\Xi(\boldsymbol{\theta})$ and $\Phi_h(\boldsymbol{\eta})$ the feasible regions of the variables in the high-level and low-level components, respectively. In particular, $\Xi(\boldsymbol{\theta})$ is defined by the set of constraints (5)-(6) and the high-level variable limits, while $\Phi_h(\boldsymbol{\eta})$ is defined by the set of constraints (1)-(5) and the low-level variable limits. Here, $\boldsymbol{\theta}$ collects high-level problem parameters (day-ahead offering profile, wind power generation forecast and parameters of the hydropower generation function), and $\boldsymbol{\eta}$ gathers low-level problem parameters (external inflow forecast and CRORHP parameters).

Finally, the centralized MPC problem (8) can be rewritten in the following compact form:

$$\begin{aligned}
\underset{\substack{\boldsymbol{x},\boldsymbol{p},\boldsymbol{y}_h,\\ \boldsymbol{q}_h,\bar{\boldsymbol{p}}_h,\bar{\boldsymbol{q}}_l}}{\operatorname{argmin}} \quad & J(\boldsymbol{x}) && \text{(9a)}\\
\text{s.t.} \quad & (\boldsymbol{x},\boldsymbol{p}) \in \Xi(\boldsymbol{\theta}), && \text{(9b)}\\
& (\boldsymbol{y}_h,\boldsymbol{q}_h,\bar{\boldsymbol{p}}_h,\bar{\boldsymbol{q}}_l) \in \Phi_h(\boldsymbol{\eta}), \forall l \in \boldsymbol{L}_h, \forall h \in \boldsymbol{H}, && \text{(9c)}\\
& \boldsymbol{p}_h = \bar{\boldsymbol{p}}_h : \boldsymbol{\lambda}_{\boldsymbol{p}_h}, \forall h \in \boldsymbol{H}, && \text{(9d)}\\
& \boldsymbol{q}_l = \bar{\boldsymbol{q}}_l : \boldsymbol{\lambda}_{\boldsymbol{q}_l}, \forall l \in \boldsymbol{L}_h, \forall h \in \boldsymbol{H}. && \text{(9e)}
\end{aligned}$$

We proceed by relaxing the consistency constraints using the augmented Lagrangian relaxation method. The augmented Lagrangian cost function is:

$$\begin{aligned}
L_\rho = & J + \sum_{h\in\boldsymbol{H}} \left({\boldsymbol{\lambda}_{\boldsymbol{p}_h}}^T (\boldsymbol{p}_h - \bar{\boldsymbol{p}}_h) + \frac{\rho}{2} \|\boldsymbol{p}_h - \bar{\boldsymbol{p}}_h\|_2^2 \right) + \\
& + \sum_{h\in\boldsymbol{H}} \sum_{l\in\boldsymbol{L}_h} \left({\boldsymbol{\lambda}_{\boldsymbol{q}_l}}^T (\boldsymbol{q}_l - \bar{\boldsymbol{q}}_l) + \frac{\rho}{2} \|\boldsymbol{q}_l - \bar{\boldsymbol{q}}_l\|_2^2 \right),
\end{aligned} \tag{10}$$

where ρ is a large positive parameter.

Following the APP method, we linearize the cross-terms in the augmented Lagrangian, i.e., the squared norms in (10), at the current iterate, and we add quadratic separable terms. Thanks to this linearization, at each iteration of the distributed algorithm, each component requires knowledge of the coupling variables determined by its neighboring components in the preceding iteration. This results in a full parallelization of the distributed algorithm.

The detailed implementation of the proposed distributed economic MPC strategy (DEMPC) is presented in Algorithm 1.

Algorithm 1 Distributed economic MPC (DEMPC)

Input: Parameter vectors $\boldsymbol{\theta}$ and $\boldsymbol{\eta}$

Output: Optimal control actions $\{\boldsymbol{q}_h^\star \,|\, h \in \boldsymbol{H}\}$

Initialize: $\boldsymbol{p}_h^0$, $\bar{\boldsymbol{p}}_h^0$, $\boldsymbol{q}_l^0$, $\bar{\boldsymbol{q}}_l^0$, ${\boldsymbol{\lambda}_{\boldsymbol{p}_h}}^1$, ${\boldsymbol{\lambda}_{\boldsymbol{q}_l}}^1$, ρ^1, $i \leftarrow 0$, primal residual $\boldsymbol{r}^0$, dual residual $\boldsymbol{s}^0$, $\mu \leftarrow 10$, penalty $\sigma \leftarrow 2$, tolerance $\epsilon \leftarrow 10^{-4}$, $i^{max} \leftarrow 1000$;

while $\min\left(\|\boldsymbol{r}^i\|_2, \|\boldsymbol{s}^i\|_2\right) > \epsilon$ **and** $i < i^{max}$ **do**

$i \leftarrow i + 1$;

$$\boldsymbol{x}^i, \boldsymbol{p}^i \leftarrow \underset{(\boldsymbol{x},\boldsymbol{p})\in\Xi(\boldsymbol{\theta})}{\operatorname{argmin}} \left\{ J(\boldsymbol{x}) + \sum_{h\in\boldsymbol{H}} \left({\boldsymbol{\lambda}_{\boldsymbol{p}_h}^i}^T \boldsymbol{p}_h + \right.\right.$$
$$\left.\left. + \rho^i \boldsymbol{p}_h^T \left(\boldsymbol{p}_h^{i-1} - \bar{\boldsymbol{p}}_h^{i-1}\right) + \rho^i \left\|\boldsymbol{p}_h - \boldsymbol{p}_h^{i-1}\right\|_2^2 \right) \right\};$$

$$\boldsymbol{y}_h^i, \boldsymbol{q}_h^i, \bar{\boldsymbol{p}}_h^i, \bar{\boldsymbol{q}}_l^i \leftarrow \underset{(\boldsymbol{y}_h,\boldsymbol{q}_h,\bar{\boldsymbol{p}}_h,\bar{\boldsymbol{q}}_l)\in\Phi_h(\boldsymbol{\eta})}{\operatorname{argmin}} \left\{ -{\boldsymbol{\lambda}_{\boldsymbol{p}_h}^i}^T \bar{\boldsymbol{p}}_h + \right.$$
$$-\rho^i \bar{\boldsymbol{p}}_h^T \left(\boldsymbol{p}_h^{i-1} - \bar{\boldsymbol{p}}_h^{i-1}\right) + \rho^i \left\|\bar{\boldsymbol{p}}_h - \bar{\boldsymbol{p}}_h^{i-1}\right\|_2^2 +$$
$$- \sum_{l\in\boldsymbol{L}_h} \left({\boldsymbol{\lambda}_{\boldsymbol{q}_l}^i}^T \bar{\boldsymbol{q}}_l + \rho^i \bar{\boldsymbol{q}}_l^T \left(\boldsymbol{q}_l^{i-1} - \bar{\boldsymbol{q}}_l^{i-1}\right) + \right.$$
$$\left.\left. -\rho^i \left\|\bar{\boldsymbol{q}}_l - \bar{\boldsymbol{q}}_l^{i-1}\right\|_2^2 \right) \right\};$$

Share $\left\{\boldsymbol{q}_l^i \leftarrow \bar{\boldsymbol{q}}_l^i \,|\, l \in \boldsymbol{L}_h\right\}$ with the neighbors of h;

$\boldsymbol{r}^i \leftarrow \left[\boldsymbol{p}_h^i - \bar{\boldsymbol{p}}_h^i, \boldsymbol{q}_l^i - \bar{\boldsymbol{q}}_l^i\right]^T$;

$\boldsymbol{s}^i \leftarrow \rho^i \left[\bar{\boldsymbol{p}}_h^i - \bar{\boldsymbol{p}}_h^{i-1}, \bar{\boldsymbol{q}}_l^i - \bar{\boldsymbol{q}}_l^{i-1}\right]^T$;

$\left[{\boldsymbol{\lambda}_{\boldsymbol{p}_h}^{i+1}}, {\boldsymbol{\lambda}_{\boldsymbol{q}_l}^{i+1}}\right]^T \leftarrow \left[{\boldsymbol{\lambda}_{\boldsymbol{p}_h}^{i}}, {\boldsymbol{\lambda}_{\boldsymbol{q}_l}^{i}}\right]^T + \rho^i \boldsymbol{r}^i$;

if $\|\boldsymbol{r}^i\|_2 > \mu \|\boldsymbol{s}^i\|_2$ **then** $\rho^{i+1} \leftarrow \sigma\rho^i$;

else if $\|\boldsymbol{s}^i\|_2 > \mu \|\boldsymbol{r}^i\|_2$ **then** $\rho^{i+1} \leftarrow \frac{1}{\sigma}\rho^i$;

else $\rho^{i+1} \leftarrow \rho^i$;

end while

The APP method has been extensively researched and theoretically validated for convex problems [20]. Despite lacking this theoretical foundation for problems involving integer constraints, this approach often serves as effective heuristics, offering both upper and lower bounds along with feasible solutions [21].

In essence, the drawback of a heuristic compared to a global method is straightforward: it may not yield an optimal point. Yet, the advantage lies in its potential for significantly faster execution than a global method, a characteristic particularly beneficial in numerous practical applications. Specifically for the present problem, model (8) already encompasses several approximations of the nonlinear physical dynamics inherent to the VPP. Consequently, further pursuit of global optimization may not be justified considering the additional effort it entails. Furthermore, the proposed approach aims to furnish a rapid tool for optimizing the global economic key performance indicators of the VPP. In practical scenarios, the outcome of Algorithm 1 will not directly translate into the actual commands executed in real-time. Rather, it will function as an economic signal employed as a reference by dedicated local controllers, which can be leveraged to accommodate the nonlinear dynamics of each asset.

It is worth mentioning that a straightforward approach to

recover the global convergence conditions for APP involves relaxing the integer constraints and subsequently rounding to achieve integrality upon termination. However, this technique frequently yields poor-quality solutions in many practical applications [22].

IV. Simulation Results and Discussion

In this section, we present simulation results covering a three months period (February-April 2017). This timeframe encompasses diverse water inflow conditions, enabling a comprehensive exploration of various scenarios encountered by the VPP. The parameters employed in the simulations can be found in Table I. Simulations are performed using historical time series of DAM prices in France. The MPC runs with control intervals of 10 minutes and a prediction horizon of 24 hours. The algorithm is implemented on a computer equipped with an Intel i7 processor, utilizing Gurobi 9.5.0 as the solver.

TABLE I
Parameters of the simulations.

Type	Parameter	Value
Market	Hourly average $\pi^{E,\downarrow}; \pi^{E,\uparrow}$	$57.32; 32.81$ (€/MWh)
Wind	Hourly average wind power	66.54 (MW)
Hydro	$Q_{tr}^{min}(1); Q_{tr}^{min}(2); Q_{tr}^{min}(3)$	$110; 60; 140$ (m^3/s)
	$Q_{tr}^{max}(1); Q_{tr}^{max}(2); Q_{tr}^{max}(3)$	$1600; 1500; 2220$ (m^3/s)
	$Q_{br}^{min}(1); Q_{br}^{min}(2); Q_{br}^{min}(3)$	$80; 56; 72$ (m^3/s)
	$\Delta Q_{tr}(1); \Delta Q_{tr}(2); \Delta Q_{tr}(3)$	$125; 150; 200$ (m^3/s)
	$\tau_{1,2}^{tr}; \tau_{2,3}^{tr}; \tau_{3,4}^{tr}; \tau_{1,2}^{br}; \tau_{2,3}^{br}; \tau_{3,4}^{br}$	$300; 0; 0; 300; 0; 300$ (s)
	$S(1); S(2); S(3)$	$6.13; 5.95; 5.34$ (Km^2)
	Hourly average water inflow	1168.64 (m^3/s)

In Fig. 4, we present an illustrative example showing the daily operation of the last hydropower system in the CRORHP, when our DEMPC is employed. As the operation of the last development hinges on the decisions made for the upstream developments, this analysis offers valuable insights into the integrated operation of the entire CRORHP. During peak price periods, the reservoir is strategically depleted to seize these favorable market opportunities. Note that the reservoir storage capacity is tied to the inflow, as depicted in Fig. 2. This inflow, in turn, depends on the outflow of the upstream developments. Hence, the distributed controller effectively orchestrates the actions of the upstream developments to guarantee that full storage capacity is available during peak price periods.

In Fig. 4 we can also observe the impact of incorporating direct knowledge of the aggregator economic key performance indicators into the control strategy. When the water level attains its maximum, constraint (4) is satisfied, allowing the opening of the barrage. Nevertheless, this proves economically inefficient as the turbines have not yet reached their full capacity. Thus, the barrage remains closed. This behavior directly results from the formulation of the objective (7), which models the economic goal of the aggregator (economic MPC), rather than merely minimizing the mismatch between a set-point and the actual dispatch, as in traditional MPC.

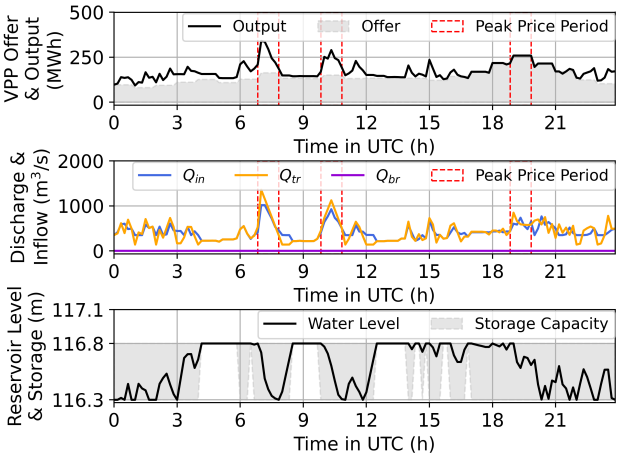

Fig. 4. Example of daily operation of the last hydropower system in the hydropower cascade.

To assess the ability of DEMPC in enhancing the market value of the VPP, we compare it to two alternative approaches:

- *Uncoordinated economic MPC* (UEMPC), which dispatches the CRORHP and wind independently in the DAM.
- *Ideal control*, which solves the centralized dispatch problem (8) using the actual uncertainty realization instead of forecasts.

Table II summarizes this comparison.

TABLE II
Ex-post energy imbalances and revenue for various dispatch strategies. Hourly average values normalized by VPP power generation. In brackets, the relative difference with respect to UEMPC.

Strategy	Positive imb. (MWh/MWh)	Negative imb. (MWh/MWh)	Revenue (€/MWh)
UEMPC	0.13	0.10	37.22
DEMPC	0.10 (**−23%**)	0.07 (**−30%**)	37.93 (**+1.9%**)
Ideal control	0.07 (−46%)	0.05 (−50%)	38.69 (+3.9%)

The variations in Table II arise solely from different time of use of the reservoirs. In fact, the final VPP energy generation is independent from the dispatch strategy, since wind power is uncontrollable and hydropower depends solely on the inflow. Compared to UEMPC, our DEMPC exhibits a 1.9% revenue increase, which shows that the coalition of hydropower and wind improves the market value of both assets. Compared to the ideal controller, our DEMPC shows a 2% revenue decrease. Extending the MPC prediction horizon could narrow this gap, albeit at the expense of heightened model complexity. The net hourly revenues observed with UEMPC, DEMPC, and ideal control stand at approximately 12211€/h, 12454€/h and 12689€/h, respectively. Extrapolating the findings of this simulation to an entire year, employing our DEMPC rather than individually dispatching VPP resources via UEMPC, would yield an estimated annual revenue increase of approximately €2.13 million.

The revenue increase achieved when jointly optimizing hydropower and wind depends on the CRORHP effectiveness in mitigating wind variability. However, unlike batteries, the storage capacity of the CRORHP is variable and reliant on the inflow from the river and its tributaries (see Fig. 5).

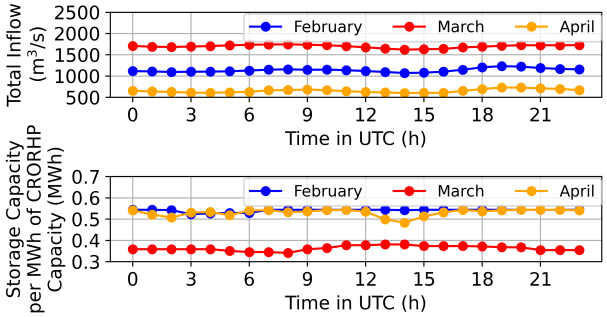

Fig. 5. Average daily water inflow and corresponding storage capacity of the hydropower cascade.

Table III shows the impact of inflow seasonality on the revenue of the aggregator. During normal inflow conditions (February and April), the joint dispatch yields significant revenue increases ($+1.9\%$ and $+2.5\%$, respectively) compared to the independent dispatch strategy. Conversely, during flood periods (March), the CRORHP is compelled to operate mostly in a pure run-of-the-river mode, with no storage capacity. In this case, the difference between joint and independent dispatch narrows significantly. This clearly shows that run-of-the-river ability to mitigate RES fluctuations is directly linked to the inflow seasonality, which, in turn, dictates the storage capacity of the reservoirs.

TABLE III
EX-POST REVENUE WITH INDEPENDENT (UEMPC) AND JOINT (DEMPC) HYDRO-WIND DISPATCH. HOURLY AVERAGE VALUES NORMALIZED BY VPP POWER GENERATION. IN BRACKETS, THE RELATIVE DIFFERENCE WITH RESPECT TO UEMPC.

Strategy	**Revenue (€/MWh)**		
	February	**March**	**April**
UEMPC	47.63	33.41	31.52
DEMPC	48.54 (**+1.9%**)	33.70 (**+0.9%**)	32.32 (**+2.5%**)

Numerical results comparing the computational performances of the centralized and distributed approaches are shown in Table IV. Compared to centralized MPC, our distributed MPC reduces by $\sim 10\%$ the average time required to solve one step of the controller with more than 99% accuracy.

A notable drawback of distributed algorithms is their sensitivity to parameters tuning. To delve deeper into this issue, Fig. 6 reports the computational performances of our DEMPC when varying both the penalty parameter σ and the tolerance parameter ϵ. When σ is set to low values, our DEMPC outperforms centralized MPC in terms of time required to solve the VPP dispatch. However, poor tuning of σ is shown to increase significantly the MPC execution time, potentially nullifying the computational advantage achieved through the decomposition. Also, Fig. 6 reveals an inherent trade-off

TABLE IV
COMPUTATIONAL PERFORMANCES. THE ERROR IS COMPUTED RELATIVE TO THE OBJECTIVE FUNCTION VALUE OF THE CENTRALIZED MPC.

Quantity	**Centralized MPC**			**Distributed MPC**		
	Mean	**Std**	**Max**	**Mean**	**Std**	**Max**
Relative error (%)	-	-	-	0.48	0.91	1.96
Iteration time (s)	-	-	-	0.41	0.36	1.56
Iterations count (-)	-	-	-	23.21	3.81	30
MPC step time (s)	10.58	6.58	27.31	9.51	5.67	26.86

between controller execution time and accuracy. Lower values of ϵ necessitate more iterations for DEMPC convergence but increase its precision. Nevertheless, once a certain threshold is crossed ($\epsilon = 10^{-4}$ in this case), we observe an exponential surge in the execution time, yielding only negligible improvements in the accuracy. Established guidelines for optimizing parameters tuning are available [20].

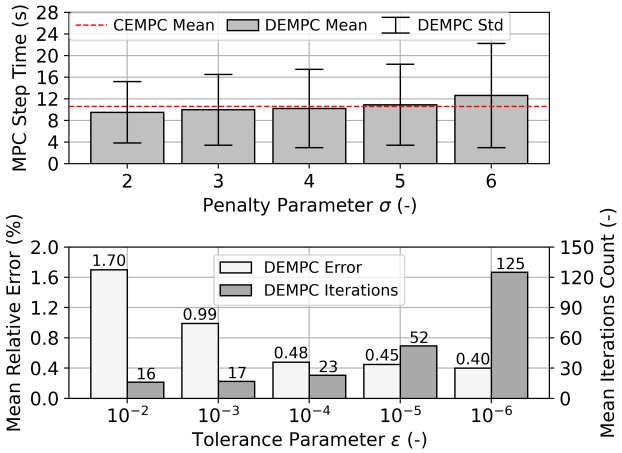

Fig. 6. DEMPC sensitivity to parameters tuning.

V. CONCLUSIONS AND FUTURE WORK

In this study, we present a control strategy for the joint energy dispatch of wind farms and a CRORHP. As a distinct feature, the strategy is fully-distributed, eliminating the need for a central coordinator. Decentralization not only enhances the scalability of the controller but also fortifies its robustness to communication failures and enables the integration of privacy-preserving techniques, particularly when VPP assets are managed by distinct owners. By partnering with the French aggregator Compagnie Nationale du Rhône, we evaluate the proposed approach on a complex case study. Compared to centralized MPC, our distributed controller reduces by $\sim 10\%$ the average time needed to optimize the VPP dispatch. Furthermore, the joint dispatch of wind and run-of-the-river hydropower is shown to improve by $\sim 2\%$ the revenue of the aggregator, compared to operating these resources independently in the market.

Future research directions entail expanding our evaluation to the full-scale case study of Compagnie Nationale du Rhône (19 hydropower systems), and develop control algorithms that

explicitly accounts for the nonlinear dynamics of the cascaded hydropower system. Furthermore, alongside the proposed sensitivity analyses, investigating the scalability of the distributed method when varying the number of controllable assets in the VPP, and consequently the number of nodes and edges in the underlying distributed network, could lead to a more comprehensive assessment of the proposed approach.

REFERENCES

[1] J. F. Venegas-Zarama, J. I. Muñoz-Hernandez, L. Baringo, P. Diaz-Cachinero and I. De Domingo-Mondejar, "A review of the evolution and main roles of virtual power plants as key stakeholders in power systems," *IEEE Access*, vol. 10, pp. 47937-47964, 2022.

[2] N. Naval and J. M. Yusta, "Virtual power plant models and electricity markets - A review," *Renewable and Sustainable Energy Reviews*, vol. 149, pp. 111393, 2021.

[3] S. Camal, A. Michiorri and G. Kariniotakis, "Optimal Offer of automatic frequency restoration reserve from a combined PV/wind virtual power plant," *IEEE Transactions on Power Systems*, vol. 33, no. 6, pp. 6155-6170, 2018.

[4] L. Berga, "The role of hydropower in climate change mitigation and adaptation: A review," *Engineering*, vol. 2, no. 3, pp. 313-318, 2016.

[5] International Energy Agency (2021), "Hydropower special market report – analysis," IEA, https://www.iea.org/reports/hydropower-special-market-report (accessed August, 2023).

[6] B. François, B. Hingray, D. Raynaud, M. Borga and J.D. Creutin, "Increasing climate-related-energy penetration by integrating run-of-the river hydropower to wind/solar mix," *Renewable Energy*, vol. 87, pp. 686-696, 2016.

[7] R. Sioshansi, "Optimized offers for cascaded hydroelectric generators in a market with centralized dispatch," *IEEE Transactions on Power Systems*, vol. 30, no. 2, pp. 773-783, 2015.

[8] Y. Yu, Y. Wu and Q. Sheng, "Optimal scheduling strategy of cascade hydropower plants under the joint market of day-ahead energy and frequency regulation," *IEEE Access*, vol. 9, pp. 87749-87762, 2021.

[9] J. Zhang, C. Cheng, S. Yu and H. Su, "Chance-constrained co-optimization for day-ahead generation and reserve scheduling of cascade hydropower–variable renewable energy hybrid systems," *Applied Energy*, vol. 324, pp. 119732, 2022.

[10] Y. Qiu, J. Lin, F. Liu, Y. Song, G. Chen and L. Ding, "Stochastic online generation control of cascaded run-of-the-river hydropower for mitigating solar power volatility," *IEEE Transactions on Power Systems*, vol. 35, no. 6, pp. 4709-4722, 2020.

[11] G. Hug-Glanzmann, "Predictive control for balancing wind generation variability using run-of-river power plants," in *2011 IEEE Power and Energy Society General Meeting*, Detroit, MI, USA, 2011, pp. 1-8.

[12] D. I. Hidalgo-Rodríguez and J. Myrzik, "Optimal operation of interconnected home-microgrids with flexible thermal loads: A comparison of decentralized, centralized, and hierarchical-distributed model predictive control," in *2018 Power Systems Computation Conference (PSCC)*, Dublin, Ireland, 2018, pp. 1-7.

[13] R. Gupta, F. Sossan, E. Scolari, E. Namor, L. Fabietti, C. Jones and M. Paolone, "An ADMM-based coordination and control strategy for PV and storage to dispatch stochastic prosumers: Theory and experimental validation," in *2018 Power Systems Computation Conference (PSCC)*, Dublin, Ireland, 2018, pp. 1-7.

[14] D. K. Molzahn, F. Dörfler, H. Sandberg, S. H. Low, S. Chakrabarti, R. Baldick and J. Lavaei, "A survey of distributed optimization and control algorithms for electric power systems," *IEEE Transactions on Smart Grid*, vol. 8, no. 6, pp. 2941-2962, 2017.

[15] A. Maneesha and K. S. Swarup, "A survey on applications of Alternating Direction Method of Multipliers in smart power grids," *Renewable and Sustainable Energy Reviews*, vol. 152, pp. 111687, 2021.

[16] G. Cohen, "Auxiliary problem principle and decomposition of optimization problems," *Journal of Optimization Theory and Applications*, vol. 32, pp. 277-305, 1980.

[17] V. Piron, G. Bontron and M. Pochat, "Operating a hydropower cascade to optimize energy management," *Hydropower & Dams*, vol. 22, no. 5, pp. 2-6, 2015.

[18] M. Yuhang, H. Yuan, W. Gang, L. Junyong, L. Yang, X. Yue, L. Youbo and T. Zao, "Decentralized monthly generation scheduling of cascade hydropower plants in multiple time scale markets," *International Journal of Electrical Power & Energy Systems*, vol. 135, pp. 107420, 2022.

[19] A. V. Ntomaris, I. G. Marneris, P. N. Biskas and A. G. Bakirtzis, "Optimal participation of RES aggregators in electricity markets under main imbalance pricing schemes: Price taker and price maker approach," *Electric Power Systems Research*, vol. 206, pp. 107786, 2022.

[20] S. Boyd, N. Parikh, E. Chu, B. Peleato and J. Eckstein, "Distributed optimization and statistical learning via the alternating direction method of multipliers," *Foundations and Trends in Machine learning*, vol. 3, no.1, pp. 1-122, 2011.

[21] R. Takapoui, N. Moehle, S. Boyd and A. Bemporad, "A simple effective heuristic for embedded mixed-integer quadratic programming," in *2016 American Control Conference (ACC)*, Boston, MA, USA, 2016, pp. 5619-5625.

[22] JP. Watson and D. L. Woodruff, "Progressive hedging innovations for a class of stochastic mixed-integer resource allocation problems," *Computational Management Science*, vol. 8, pp. 355–370, 2011.